

# Weinberg Angle, Neutron Abundance in BBN, and Lifetime

Cheng Tao Yang , and Johann Rafelski 

Department of Physics, The University of Arizona, Tucson, Arizona 85721, USA

## Abstract

The Big-Bang nucleosynthesis (BBN) initial neutron abundance and the neutron lifetime depend on the magnitude of the Fermi coupling constant  $G_F$ . When allowing for radiative corrections,  $G_F$  depends on the symmetry breaking Weinberg angle  $s_W$ , a free parameter in the standard model of particle physics which could have considerable environmental (e.g. cosmological or temperature) dependence. We establish how the value of  $s_W$  influences BBN and neutron lifetime.

**Keywords:** Neutron Abundance in BBN; Weinberg Angle; Fermi Constant; Neutron Lifetime

## 1. Introduction

The primary motivation for this work is to quantify the primordial neutron abundance and thus the outcome of the Big-Bang nucleosynthesis (BBN) dependence on the (temperature) variation of the Fermi interaction constant  $G_F$ . There is continued interest in understanding the cosmological variation of natural constants [1], with much of recent interest arising in the context of the Hubble tension [2]. We studied this context before, exploring the dependence of neutrino freeze-out on the variation of natural constants [3] in the primordial Universe. Our present work extends these considerations to the domain of BBN nucleosynthesis physics. Our motivation here is more general; we expect  $G_F$  to be significantly influenced by way of  $s_W$  by the pre-BBN plasma temperature.

$G_F$  and thus the relevant weak interaction (WI) reaction rates, allowing for higher radiative corrections, become dependent on a few parameters of the Standard Model (SM) of particle physics. We expect, see Section 2, that the relevant to nucleosynthesis primordial Universe variation in value of  $G_F$  could originate in the value of the symmetry breaking Weinberg angle parameter used in the convenient form  $s_W \equiv \sin^2 \theta_W$ ,  $c_W \equiv \cos^2 \theta_W$ . Our secondary objective is to use the same method to popularize the dependence of the neutron lifetime on this symmetry breaking parameter of electro-weak interactions.

The WI Fermi coupling constant at tree level [4]  $G_F^{\text{tree}} = 1/\sqrt{2}v^2$  is only dependent on the Higgs vacuum expectation value  $\langle h \rangle \equiv v$ , where  $v = 246.2 \text{ GeV}$  and  $1/\sqrt{2}v^2 = 1.1665 \times 10^{-5} \text{ GeV}^{-2}$ . This is the dependence we considered in the prior study of natural constants [3]. However, through radiative vacuum polarization type correction to the charged current mediating  $W$ -Boson [4] one finds to leading order [5,6]

$$G_F = \frac{1}{\sqrt{2}v^2} \left( 1 + \Delta\alpha - \frac{c_W}{s_W} \Delta\rho + \Delta r_{\text{rem}} \right), \quad (1)$$

where  $\Delta\alpha$  is the fine-structure constant radiative correction,  $\Delta\rho$  is the charged current gauge  $W$ -boson vacuum polarization correction, and  $\Delta r$  includes sub-leading corrections.

Received:

Revised:

Accepted:

Published:

**Copyright:** © 2026 by the authors.

Submitted to *Particles* for possible open access publication under the terms and conditions of the [Creative Commons Attribution \(CC BY\) license](https://creativecommons.org/licenses/by/4.0/).

[Creative Commons Attribution \(CC BY\) license](https://creativecommons.org/licenses/by/4.0/).

In Section 2.1 we look closer at the Weinberg angle, discuss its possible and relevant for this work dependence on ambient properties such as temperature and external fields. In Section 2.2 we discuss further the Fermi constant and its electro-weak radiative corrections, highlighting its dependence on the Weinberg angle. We show, somewhat unexpected, how a small variation in  $s_W$  through its effect on  $G_F$  modifies in a noticeable manner WI reaction rates.

We review the theory and experiment on neutron lifetime in Section 3.1. In Section 3.2 we study how the primordial plasma medium in the Universe modifies the neutron lifetime by blocking the decay phase space. Combining this with the thermal model and neutron decay during the 200 seconds to reach the onset of BBN at  $T \approx 0.07$  MeV, one obtains a first view of expected neutron abundance in the Universe [7].

The study of Fermi blocking introduced the general method of approach allowing the study of neutron and proton reactions on the lepton Universe background, see Section 4.2. The freeze-out of neutron abundance turns out to require a study of the kinetic population equation to understand precisely the neutron abundance which we address in Section 4.3. This more refined understanding of the role of electro-weak processes in a kinetic model allows us to quantify the dependence of the neutron abundance on the actual primordial value of the Weinberg angle.

To obtain precise neutron abundance we need to have a precise understanding of the ratio of weak interaction strength to the Hubble expansion rate  $H$ , which we discuss in Appendix A based on our recent work [8]. We show the precise dependence of  $H$  on the baryon and entropy content, usually stated in form of baryon to photon ratio  $\eta_b$ , and the number of neutrino species  $N_\nu$ , which is near but above the value three, since by definition it comprises an inflow of entropy due to pre-freeze-out neutrino reheating by electron-positron annihilation. We conclude this work with discussion of the implications of our results in Section 5.

## 2. Electroweak Theory Parameters

### 2.1. Weinberg angle

In some beyond standard model (BSM) theoretical models, the magnitude of the electro-weak symmetry breaking is predicted and thus the value of  $s_W$  is fixed. This is not the case in SM where  $s_W$  is a free parameter. The value may be associated with the lowest vacuum energy configuration. However such a theoretical determination awaits.

The value of  $s_W$  controls the splitting in mass of the gauge Bosons  $W, Z$  and yet it appears in the WI dominating charged current interactions mediated by  $W$  only in beyond the tree level radiative corrections, see Eq. (1). Given this situation we expect that any future dynamic theory determining the value of  $s_W$  by seeking the minimum of an effective action includes similar in magnitude effects of both charged and neutral currents contributions to the vacuum energy. At the time of writing, there is nothing in literature we could find that would offer evaluation of radiative corrections as the origin of the Weinberg angle and no reference could be found addressing the temperature dependence. The work which followed on the foundational in this context work of Coleman and Weinberg [9] appears to address unrelated question.

Since these questions are not yet addressed in the literature we advance intuitive arguments: Given the radiative dependence of  $G_F$  on  $s_W$ , the minimum in effective potential as a function of  $s_W$  obtained at radiative level could be governed by much lower energy scale compared to the usual in the SM. This is so seen the required radiative factors  $\alpha^{2n}$ . Therefore the value of the Weinberg angle and thus  $G_F$  would be unusually sensitive to the environmental conditions including temperature, and external (strong) fields. Seen

from another perspective: Symmetry breaking in quantum mechanics is predominantly a function of the environmental conditions. Elementary are Zeeman and Stark effect.

The experimental value of the Weinberg angle is discussed in Ref. [6,10]  $s_W^Z \equiv \sin^2 \theta(m_Z)_W = 0.2313$ . This value relates to experimental data obtained in experiments near to the indicated scale  $m_Z$ , the mass of the Z-gauge meson mediating neutral current. Yet a somewhat larger value  $s_W^0 = 0.238$  for a lower energy scale is suggested by recent global result analysis [11]. The more recently reported LHCb [12] and CMS [13] results agree. However, the recommended NIST-CODATA value [14] we adopt in this work addressing low energy phenomena is smaller,  $s_W = 0.223$ . The difference between these two low energy values is nearly 7%. Even when allowing for the difference in scales one cannot but wonder if a variation in  $s_W$  is not due to additional uncontrolled factors characterizing the experimental setups: The value of  $s_W$  could, for example, be dependent in a sensitive manner on external electromagnetic fields. This could help us understand why different experiments obtain not fully concordant values of the Weinberg angle. We will see that a much smaller variance in  $s_W$  suffices to explain the disagreement in the measured values of neutron lifetime.

We believe that the value of the symmetry breaking Weinberg angle can change at percent-level for temperature as low as a fraction of a MeV given the theoretical considerations, without contradicting any experimental result. This is so since as discussed the minimum in vacuum energy as a function of Weinberg angle is probably flat. Therefore it seems appropriate to explore sensitivity of BBN to modest modification of  $s_W$ , also as a motivation for future study of the SM effective potential as a function of  $s_W$ .

More generally, the finite temperature could, in principle, influence the value of the vacuum expectation value  $v$  of the Higgs field. This requires temperatures which are above 20 GeV as we will address in quantitative manner in near future. Computation of this effect is possible since action of the SM has a well defined minimum as a function of  $v$ . As discussed we do not know the shape of the minimum in vacuum energy as function of Weinberg angle and a dynamical theory was not developed.

To conclude:

- We believe that the effective electro-weak vacuum energy minimum as a function of  $s_W$  is relatively shallow rendering the value susceptible to modification by environmental factors;
- In the primordial Universe the effective value of the Weinberg angle  $s_W$  can differ from its low-energy laboratory value due to the thermal plasma background effects. As a result, the Fermi constant  $G_F$  in this environment could acquire a temperature dependent shift.
- We consider it possible that value of the Weinberg angle  $s_W$  is different in different experimental environments in the presence of strong electromagnetic fields, which could result in method dependent neutron lifetime measurement.

## 2.2. Fermi constant: Radiative corrections

In this section we explore the sensitivity of the effective Fermi constant to variations in the Weinberg angle. Within the Standard Model, the most precise value of the Fermi constant Eq. (1) was obtained from precisely measured muon lifetime [15]  $G_F^\mu = 1.1663787(6) \times 10^{-5} \text{ GeV}^{-2}$ .  $G_F$  can be written using measured quantities in the form [10,16]

$$G_F = \frac{\pi\alpha}{\sqrt{2}m_W^2 s_W} (1 + \Delta r), \quad \text{where in SM} \quad e^2 = g^2 s_W, \quad m_W^2 = g^2 \frac{v^2}{4}. \quad (2)$$

In the temperature range considered here,  $1 > T > 0.01$  MeV, we take the Higgs field vacuum expectation value  $v = 246.2$  GeV to be a constant. The radiative corrections are summarized in the quantity  $\Delta r$ . The quantum correction  $\Delta r$  has seen extensive theoretical study. The one-loop correction can be written as [6,17]

$$\Delta r = \Delta\alpha - \frac{c_W}{s_W} \Delta\rho + \Delta r_{\text{rem}}, \quad (3)$$

where  $\Delta\alpha$  is the correction due to the running of fine-structure constant  $\alpha$ ; we have

$$\Delta\alpha = \frac{\hat{\alpha}(m_Z) - \alpha}{\hat{\alpha}(m_Z)} \approx 0.06654. \quad (4)$$

The second term  $\Delta\rho$  quantifies how neutral-current and charged-current interactions are modified by the loop effect. The leading contribution to  $\Delta\rho$  arises from the mass splitting between the top and bottom quarks and depends quadratically on the top-quark mass, we have [18]

$$\Delta\rho = \frac{3 G_F m_t^2}{8\sqrt{2}\pi^2} = \frac{3 G_F}{8\sqrt{2}\pi^2} \left( \frac{g_t v}{\sqrt{2}} \right)^2, \quad (5)$$

where we rewrite the top quark mass in terms of vacuum expectation value; we have  $m_t = g_t v / \sqrt{2}$  with top quark coupling constant  $g_t \approx 1$ . The remainder term  $\Delta r_{\text{rem}}$  contains sub-leading contributions, including the dependence on the Higgs-boson mass. Numerically, its impact is small, contributing at the  $\sim 1\%$  level [17].

In the following calculation, the remainder term is negligible; we thus obtain a self-consistent Dyson-like equation for the Fermi constant:

$$G_F = \frac{1}{\sqrt{2}v^2} \left( 1 + \Delta\alpha - \frac{c_W}{s_W} \frac{3G_F}{8\sqrt{2}\pi^2} \frac{v^2}{2} \right). \quad (6)$$

We can solve in self-consistent manner

$$G_F^{\text{sum}} = \frac{1}{\sqrt{2}v^2} \left( \frac{1 + \Delta\alpha}{1 + 3c_W/32\pi^2 s_W} \right). \quad (7)$$

However, this is an infinite series and very likely higher order terms are not consistently accounted for. Therefore we will consider the 1st perturbative modification

$$G_F^{1\text{st}} \approx \frac{1}{\sqrt{2}v^2} \left( 1 + \Delta\alpha - \frac{3c_W}{32\pi^2 s_W} \right). \quad (8)$$

From experimental measurements, the experimental Fermi constant value is defined at the measured value of  $s_W$

$$G_F^{\text{exp}} = G_F|_{s_W=0.223(\text{measured})}. \quad (9)$$

In Fig. 1, we quantify the dependence of the normalized Fermi constant  $(G_F/G_F^{\text{exp}})^2$  on the Weinberg angle in the range  $0.21 < s_W < 0.24$ . The impact of even a small variations in the Weinberg angle on the Fermi constant  $G_F^2$  is non-negligible. We note that the presented range of  $s_W$  can account for the observed sub-percent discrepancy in neutron lifetime. This demonstrates that precision measurements of neutron decay are sensitive probes of electro-weak parameters and that even slight shifts in the Weinberg angle could have measurable effects on weak interaction processes.

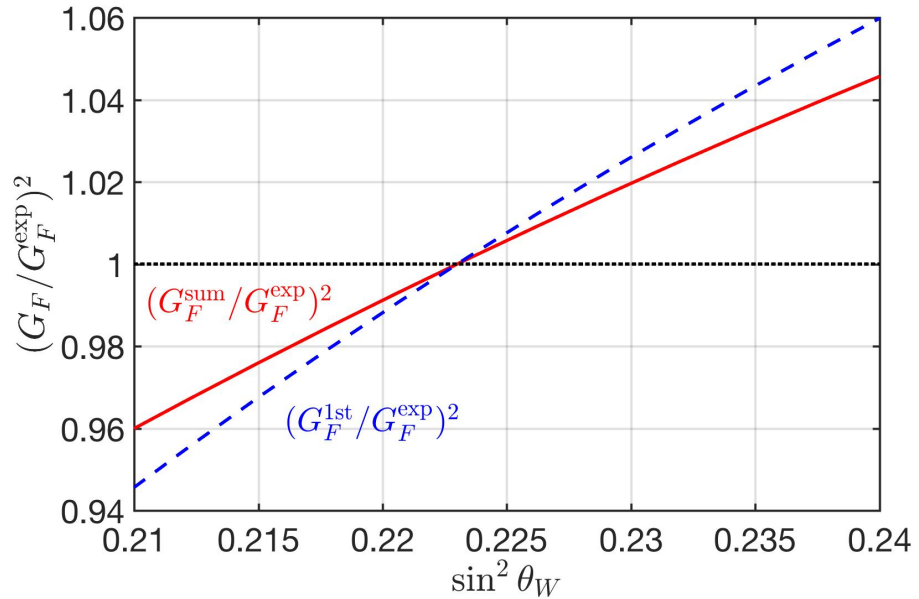


**Figure 1.** The normalized Fermi constant  $(G_F/G_F^{\text{exp}})^2$  as a function of the Weinberg angle  $s_W$  within the range  $0.21 < s_W < 0.24$ . The horizontal dotted line indicates the standard-model value  $G_F = G_F^{\text{exp}}$ . The two methods of treating the radiative corrections are discussed in text.

### 3. Neutron Decay Rate

#### 3.1. Decay in vacuum

For the neutron decay channel

$$n \longrightarrow p + e + \bar{\nu}_e, \quad (10)$$

the vacuum lifetime of neutron can be written as:

$$\frac{1}{\tau_n^0} = \frac{1}{2m_n} \int \frac{d^3 p_{\bar{\nu}}}{(2\pi)^3 2E_{\bar{\nu}}} \frac{d^3 p_p}{(2\pi)^3 2E_p} \frac{d^3 p_e}{(2\pi)^3 2E_e} (2\pi)^4 \delta^4(p_n - p_p - p_e - p_{\bar{\nu}}) \langle |\mathcal{M}|^2 \rangle, \quad (11)$$

where the invariant matrix element for the neutron decay for non-relativistic neutron and proton is given by

$$\langle |\mathcal{M}|^2 \rangle \approx 16 G_F^2 V_{ud}^2 m_n m_p (1 + 3g_A^2) E_{\bar{\nu}} E_e. \quad (12)$$

The neutron lifetime is seen proportional to several parameters; the textbook final result is [20–23]

$$\Gamma_n^0 = \frac{G_F^2 V_{ud}^2 Q^5}{2\pi^3} (1 + 3g_A^2) \mathcal{F} f = D \mathcal{F} f, \quad (13)$$

where the phase space factor  $f$  is

$$f \equiv \int_{m_e/Q}^1 d\zeta \zeta (1 - \zeta)^2 \sqrt{\zeta^2 - \left(\frac{m_e}{Q}\right)^2} = 0.01575. \quad (14)$$

This factor  $f$  varies from reaction to reaction and in medium; hence we separated out the reaction strength  $D$  appearing here and below in all (thermal) reaction rates allowing to write

$$\Gamma' = \Gamma/D, \quad D = \frac{G_F^2 V_{ud}^2 Q^5}{2\pi^3} (1 + 3g_A^2). \quad (15)$$

$Q$  is the neutron-proton mass difference

$$Q = m_n - m_p = 1.2933324(5) \text{ MeV}. \quad (16)$$

When more than 5 digits precision are needed, the more accurate form reads

$$Q = (m_n - m_p) \left[ 1 - \frac{m_n - m_p}{2m_n} \left( 1 - \frac{m_e^2}{(m_n - m_p)^2} \right) \right]. \quad (17)$$

The nucleon structure enters Eq. (13) in terms of  $g_A = 1.2755$ , the ratio of transition axial current to transition vector current. The electro-weak structure is encoded in the weak Fermi coupling  $G_F$  and  $V_{ud}$ , the Cabibbo-Kobayashi-Maskawa (CKM) flavor mixing between down and up quarks  $V_{ud}^2 = 0.974$ . We further included in Eq. (13) the Coulomb correction between electron and proton, proton recoil, nucleon size correction etc. achieved by the additional factor [19,20,23]  $\mathcal{F} = 1.0322$ .

In total the theoretical decay rate compares well to the experimental result: The neutron lifetime has been measured with high precision in laboratory experiments using two approaches, the bottle method and the beam method. In the former neutrons are trapped and the surviving neutrons are counted with varying storage times. In the beam method, observed detection rate of the decay products gives the neutron decay rate. The beam method [24] (two experimental results) gives an average lifetime of  $\tau_n^{\text{beam}} = 888.1 \pm 2.0$  sec, while the trap method (8 experimental results since 1990) gives  $\tau_n^{\text{trap}} = 878.36 \pm 0.45$  sec [25]. The Particle Data Group [6] (PDG-2024) presents as a reference value the trap value  $\tau_n^0 = 878.4 \pm 0.5$  sec disregarding, as it seems, the beam method.

Although this method-dependence of  $\tau_n^0$  may originate from unresolved experimental systematics, we recall another possible explanation: Environment dependence of the value of the symmetry breaking Weinberg angle  $s_W$ . The assumption that the value is a fixed parameter is not assured as we discussed in Section 2.1.

### 3.2. Medium effects in neutron lifespan

In this section, we explore medium effects modifying the neutron decay rate in the primordial universe. Several medium effects are negligible: We do not consider the change in mass of the proton, nor equally insignificant time dilation originating in particle thermal motion [29], as in our case, for neutrons with  $T/m < 10^{-3}$ , this effect is negligible. However, we consider the following noticeable influence on the neutron lifetime in the primordial Universe:

1. The decay Fermi blocking factors: In the relevant temperature range after neutron freeze-out  $T_f \geq T \geq T_{BBN}$ , electrons and neutrinos in the background plasma can reduce the neutron decay rate by Fermi blocking the neutron decay products, this can noticeably lengthen the neutron lifetime compared to its vacuum value. The Pauli blocking has been recognized in the literature [7,26–28], and the medium dependence of particle decay was recognized by Kuznetsova et al [29]. We use their method to quantify the ambient cosmic plasma effect on neutron decay, including as a new element the consideration of variation of  $s_W$ .
2. Gradual reheating by  $e^+e^-$ -pair annihilation: We obtain a result for  $H$  which accounts for disappearing  $e^+e^-$ -pairs in gradual manner with slowly growing difference in the

two different temperatures in cosmic plasma: In our model the already decoupled (frozen-out) neutrinos remain undisturbed. However, as the temperature decreases the thermal abundance of  $e^+e^-$ -pairs decreases and the entropy from pair annihilation feeds into photons and charged particles, leading to reheating and gradually growing  $T > T_\nu$ . Gradual reheating impacts the speed of the expansion of the Universe, see Appendix A, and thus neutron abundance at the BBN epoch.

In the primordial Universe the rate of all present neutron decays per volume in medium, at finite temperature can be written as [29]

$$\frac{dW_{n \rightarrow pe\bar{\nu}}}{dVdt} = \frac{g_n}{(2\pi)^3} \int d^3p_n f_n \frac{m_n}{E_n} \left[ \frac{1}{2m_n} \int \frac{d^3p_{\bar{\nu}}}{(2\pi)^3 2E_{\bar{\nu}}} \frac{d^3p_p}{(2\pi)^3 2E_p} \frac{d^3p_e}{(2\pi)^3 2E_e} (2\pi)^4 \delta^4(p_n - p_p - p_e - p_{\bar{\nu}}) \langle |\mathcal{M}|^2 \rangle [1 - f_p] [1 - f_e] [1 - f_{\bar{\nu}}] \right], \quad (18)$$

where the phase-space factors  $(1 - f_i)$  are Fermi suppression factors in the medium. Considering the nonrelativistic neutron  $E_n \approx m_n$ , the thermal neutron decay rate per unit volume can be written as

$$\frac{dW_{n \rightarrow pe\bar{\nu}}}{dVdt} = n_n \Gamma_n. \quad (19)$$

This leads to the decay rate of one single neutron in the rest frame of the heat bath, compare Eq. (11)

$$\Gamma_n = \frac{1}{2m_n} \int \frac{d^3p_{\bar{\nu}}}{(2\pi)^3 2E_{\bar{\nu}}} \frac{d^3p_p}{(2\pi)^3 2E_p} \frac{d^3p_e}{(2\pi)^3 2E_e} (2\pi)^4 \delta^4(p_n - p_p - p_e - p_{\bar{\nu}}) \langle |\mathcal{M}|^2 \rangle [1 - f_p] [1 - f_e] [1 - f_{\bar{\nu}}]. \quad (20)$$

We employ the Fermi-Dirac distributions for the electron and the non-relativistic limit for the proton in the decay rate formula using the neutron rest frame. It is convenient to separate the proton structural factor and the electro-weak coupling described by the reaction strength  $D$ , Eq. (15) and study only the reduced reactions rates  $\Gamma'$ . The decay rate can be written using dimensionless variable  $\xi = E_e/Q$

$$\Gamma'_n = \int_{m_e/Q}^1 d\xi \frac{\xi(1-\xi)^2}{e^{-Q\xi/T} + 1} \frac{\sqrt{\xi^2 - (m_e/Q)^2}}{Y_\nu e^{-Q(1-\xi)/T_\nu} + 1}. \quad (21)$$

The neutron decay rate in the primordial Universe depends on both the photon temperature  $T$  and the neutrino effective temperature  $T_\nu$ , which is presented in Appendix A at the required level of precision.  $Q$  is the neutron-proton mass difference seen in Eqs. (16,17). The limit of the decay rate in vacuum is found in Eq. (21) ignoring the Fermi function denominators.

We do not expect that the short distance Coulomb correction between electron and proton, the proton recoil, nucleon size correction etc. are modified in the cosmic plasma. Thus we adapt the factor  $\mathcal{F}$  into our calculation at finite  $T$  and use the following neutron decay rate in the cosmic plasma

$$\Gamma_n = D\mathcal{F}\Gamma'_n \quad (22)$$

In Fig. 2, we show the ratio of the neutron lifetime in a cosmic plasma,  $\tau_n$ , to its vacuum value,  $\tau_n^0$ , as a function of plasma temperature  $T$  for three different values of the Weinberg angle,  $s_W$ . The curves indicate that at high temperatures, the neutron lifetime increases significantly relative to vacuum value due to Fermi blocking effects from the surrounding

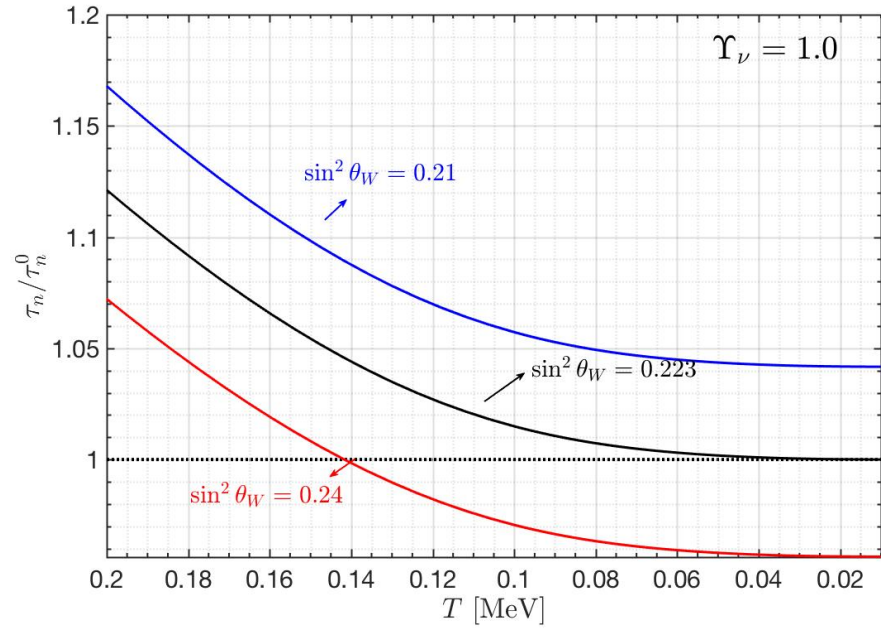


**Figure 2.** Neutron lifetime with respect to vacuum reference value  $\tau_n / \tau_n^0$  as a function of plasma temperature  $T$  for three different values of the Weinberg angle  $s_W$  with range 0.21, 0.223, 0.24.

background. As the temperature decreases towards BBN range, the ratio approaches a constant value, converging to the respective vacuum lifetime. Larger values of  $s_W$  generally correspond to longer neutron lifetimes, while smaller values lead to shorter lifetimes. This result demonstrates that even a modest variation in the electro-weak mixing angle can substantially influence neutron decay rates in the primordial plasma universe conditions, exceeding the effect of Pauli blocking.

We also note the zero-temperature limits, corresponding to the vacuum lifespan we studied in Section 3.1: The near one percent effect between beam and bottle methods is significantly smaller compared to effects shown. Consequently, some of the discrepancies observed between neutron lifetime measurements in laboratory experiments could arise from a tiny variation in the value of  $s_W$  generated by experimental environments.

## 4. Primordial BBN Neutron Concentration

### 4.1. Thermal model

In the primordial Universe we study how weak reaction rates impact the the neutron abundance at onset of BBN. We first look at a naive description: Assuming thermal equilibrium yields of particles, we define the neutron concentration  $X_n^f$  at instantaneous in temperature weak interaction (WI) freeze-out.

$$X_n^f \equiv \frac{n_n^f}{n_n^f + n_p^f} = \frac{1}{1 + e^{Q/T_f}}, \quad (23)$$

where  $n_n^f = n_n(T_f)$  and  $n_p^f = n_p(T_f)$  are freeze-out neutron and proton thermal densities, respectively, obtained at the freeze-out temperature  $T_f$ .  $X_n^f$  depends on temperature  $T_f$  at which neutrons decouple from the heat bath, and the neutron-proton mass difference (in medium)  $Q$ .

Following freeze-out, the free-streaming neutron concentration is subject only to decay

$$X_n(T_{BBN}) = X_n^f \exp\left(-\frac{t_{BBN} - t_f}{\tau_n}\right). \quad (24)$$

We see that the neutron concentration  $X_n(T_{BBN})$  provides an important probe of the underlying WI reaction rates governing the freeze-out condition, and to some extent a probe of neutron lifetime  $\tau_n$  in the primordial plasma. Normally the neutron lifetime in the vacuum,  $\tau_n \rightarrow \tau_n^0$ , is used to calculate the neutron concentration and the inputs are finessed to obtain the ‘desired’ value  $X_n(T_{BBN}) \approx 0.13$ . Many textbook presentations of BBN argue in this manner, indeed a recent study of how neutron lifespan influences BBN also took this line of thought [30], which was also present in our earlier study [27].

The above considerations require empirical input of neutron freeze-out condition and treats subsequent evolution without consideration of background scattering effects, thus provides a qualitative estimate of neutron concentration at best. The following full kinetic model study shows that these qualitative arguments do not suffice.

#### 4.2. WI Neutron and Proton Reaction Rates in the Primordial Plasma

We now show how the neutron abundance is governed by the competition between WI reaction rates governing conversion reactions between neutrons and protons, and the Hubble expansion rate. Since the Fermi constant  $G_F$  governing these rates depends on the Weinberg angle  $s_W$ , variations in this angle modify weak rates while the Hubble parameter remains set by the plasma energy density. This is the mechanism causing the BBN neutron abundance to depend on  $s_W$ .

The neutron abundance is impacted by the weak interaction reactions between neutron and proton via the dense thermal cosmic neutrino background

$$n + \nu_e \longleftrightarrow p + e^-, \quad (25)$$

$$n + e^+ \longleftrightarrow p + \bar{\nu}_e. \quad (26)$$

These are charged current reaction matrix elements mediated by the  $W$ -gauge Boson akin to the neutron decay. Therefore transition amplitudes for these nuclear reactions can be written just like those seen in the neutron decay paying attention to the momentum four-vectors of the respective reacting particles

$$|M_{n\nu \rightarrow pe}|^2 = G_F^2 V_{ud}^2 (1 + 3g_A^2) 16(p_n \cdot p_\nu)(p_p \cdot p_e), \quad (27)$$

$$|M_{ne \rightarrow p\nu}|^2 = G_F^2 V_{ud}^2 (1 + 3g_A^2) 16(p_n \cdot p_{e^+})(p_p \cdot p_\nu). \quad (28)$$

Considering the nonrelativistic limit for neutron and proton, the transition matrix becomes

$$|M_{n\nu \rightarrow pe}|^2 = G_F^2 V_{ud}^2 (1 + 3g_A^2) 16(m_n E_\nu)(m_p E_e). \quad (29)$$

$$|M_{ne \rightarrow p\nu}|^2 = G_F^2 V_{ud}^2 (1 + 3g_A^2) 16(m_n E_e)(m_p E_\nu). \quad (30)$$

The Lorentz invariant transition probability per unit time and unit volume corresponding to the process  $1 + 2 \rightarrow 3 + 4$  is

$$\frac{dW_{12 \rightarrow 34}}{dV dt} = \frac{g_1 g_2}{1 + I} \int \frac{d^3 \mathbf{p}_1}{(2\pi)^3 2E_1} \frac{d^3 \mathbf{p}_2}{(2\pi)^3 2E_2} \frac{d^3 \mathbf{p}_3}{(2\pi)^3 2E_3} \frac{d^3 \mathbf{p}_4}{(2\pi)^3 2E_4} (2\pi)^4 \delta^{(4)}(p_1 + p_2 - p_3 - p_4) |M_{12 \rightarrow 34}|^2 f_1 f_2 (1 - f_3) (1 - f_4), \quad (31)$$

where the phase-space factors  $(1 - f_i)$  are Fermi suppression factors in the medium, and the symmetry factor  $1/(1 + I)$  with  $I = 0$  for distinguishable particles in the initial states or final states, and  $I = 1$  for indistinguishable particles.

Substituting the thermal (Fermi) distribution function for the electron, the free streaming neutrino [31], nonrelativistic proton and neutron and integrating over the delta function, the thermal reaction rate per volume takes the form

$$\frac{dW_{nv \rightarrow pe}}{dV dt} = n_n \Gamma_{nv \rightarrow pe}, \quad \frac{dW_{ne \rightarrow pv}}{dV dt} = n_n \Gamma_{ne \rightarrow pv}, \quad (32)$$

where the thermal reaction rate  $\Gamma$  integrated in terms of dimensionless variables  $q = E_v/Q + 1$  and  $\eta = E_e/Q$ , respectively, are

$$\Gamma_{nv \rightarrow pe} \equiv D\Gamma'_{nv \rightarrow pe}, \quad \Gamma'_{nv \rightarrow pe} = \int_1^\infty dq \frac{q(q-1)^2 \sqrt{q^2 - (m_e/Q)^2}}{\left[1 + Y_n^{-1} e^{Q(q-1)/T_n}\right] \left[1 + e^{-Qq/T}\right]}, \quad (33)$$

$$\Gamma_{ne \rightarrow pv} \equiv D\Gamma'_{ne \rightarrow pv}, \quad \Gamma'_{ne \rightarrow pv} = \int_{m_e/Q}^\infty d\eta \frac{\eta(\eta+1)^2 \sqrt{\eta^2 - (m_e/Q)^2}}{\left[1 + Y_n e^{-Q(\eta+1)/T_n}\right] \left[1 + e^{Q\eta/T}\right]}. \quad (34)$$

For the reverse reaction, the Lorentz invariant transition probability per unit time and unit volume corresponding to the given reactions can also be written as above

$$\frac{dW_{pe \rightarrow nv}}{dV dt} = n_p \Gamma_{pe \rightarrow nv}, \quad \frac{dW_{pv \rightarrow ne}}{dV dt} = n_p \Gamma_{pv \rightarrow ne}, \quad (35)$$

where the reaction rates are given by

$$\Gamma_{pe \rightarrow nv} \equiv D\Gamma'_{pe \rightarrow nv}, \quad \Gamma'_{pe \rightarrow nv} = \int_1^\infty dq \frac{q(q-1)^2 \sqrt{q^2 - (m_e/Q)^2}}{\left[1 + Y_n e^{-Q(q-1)/T_n}\right] \left[1 + e^{Qq/T}\right]}, \quad (36)$$

$$\Gamma_{pv \rightarrow ne} \equiv D\Gamma'_{pv \rightarrow ne}, \quad \Gamma'_{pv \rightarrow ne} = \int_{m_e/Q}^\infty d\eta \frac{\eta(\eta+1)^2 \sqrt{\eta^2 - (m_e/Q)^2}}{\left[1 + Y_n^{-1} e^{Q(\eta+1)/T_n}\right] \left[1 + e^{-Q\eta/T}\right]}. \quad (37)$$

In Fig. 3 we show the thermal reaction rates as a function of temperature  $T \geq 0.01$  MeV for normal strength of WI with Weinberg angle  $\sin^2 \theta_W^2 = 0.223$ . We observe the following

- **Thermal equilibrium epoch:**  
When  $T > 1$  MeV, weak interaction rates between neutron and proton dominate Hubble rate. Since expansion of the Universe is 'slow' the neutron and proton abundances are in thermal equilibrium. Looking closer we see that the neutron-to-proton conversion decouples (becomes smaller compared to Hubble expansion) at temperature  $T \simeq 0.8$  MeV and the proton-to-neutron conversion decouples at  $T \simeq 1.3$  MeV.
- **Hubble dominance kinetic epoch:**  
Below above boundaries, in the range  $1.0 > T > 0.05$  MeV, the dominant rate is the Hubble expansion rate. In this temperature window we could naively expect that the neutron abundance only dilutes due to Universe expansion considering that all conversion reactions are smaller than the Hubble expansion rate  $H$ . In this regime, attention must be paid to the exact value of  $H$  as we encounter the transition between Hubble parameter being determined by energy density contributions of photons, neutrinos, and electrons/positrons to contributions from only photons and neutrinos driven by the smooth disappearance of  $e^\pm$ -pairs.

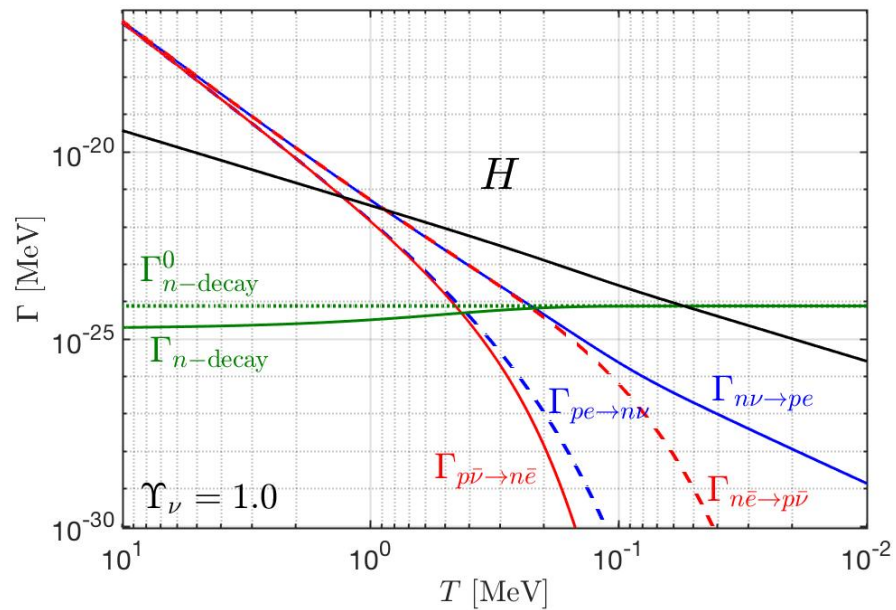


**Figure 3.** Thermal reaction rates as a function of temperature  $10 \geq T \geq 0.01 \text{ MeV}$  for processes shown in subscripts.

- **Neutron decay dominated epoch:**

When  $0.05 > T > 0.01 \text{ MeV}$  (and below), the dominant rate is the neutron decay rate, the neutron abundance is decreased by neutron decay in the primordial Universe.

In summary, there is a well-defined sequence of dominant here relevant reaction rates as the Universe cools. To accurately understand the evolution of neutron abundance in the primordial Universe, it is essential to analyze the corresponding kinetic evolution equations in detail.

#### 4.3. Kinetic Neutron Population Equation

We now develop a kinetic model for the neutron concentration, i.e. the abundance ratio between neutrons and baryons

$$X_n = \frac{N_n}{N_B} = \frac{N_n}{N_n + N_p}, \quad (38)$$

where  $N_n$  and  $N_p$  are the ‘comoving’ in the expanding volume numbers of neutron and protons respectively. The kinetic equation for the concentration of neutron can be written as

$$\frac{dX_n}{dt} = \frac{d}{dt} \left( \frac{N_n}{N_B} \right) = \frac{1}{n_B} \left( \frac{1}{V} \frac{dN_n}{dt} \right), \quad (39)$$

where we consider the comoving number of baryon is constant after the baryon genesis epoch; comoving means that we study the abundance in cosmologically expanding volumes.

The population of neutrons is governed by gains and losses due to reactions we considered

$$\frac{1}{V} \frac{dN_n}{dt} = \frac{dW_{pe \rightarrow n\nu}}{dV dt} + \frac{dW_{p\nu \rightarrow ne}}{dV dt} - \frac{dW_{n\nu \rightarrow pe}}{dV dt} - \frac{dW_{ne \rightarrow p\nu}}{dV dt} - \frac{dW_{n \rightarrow pe\nu}}{dV dt}. \quad (40)$$

Substituting the Lorentz invariant transition probability per unit time and unit volume corresponding to the given reactions, the population equation of neutrons becomes:

$$\frac{1}{V} \frac{dN_n}{dt} = n_p (\Gamma_{pe \rightarrow nv} + \Gamma_{pv \rightarrow ne}) - n_n (\Gamma_{nv \rightarrow pe} + \Gamma_{ne \rightarrow pv}) - n_n \Gamma_n. \quad (41)$$

Inserting into Eq. (39) we obtain the kinetic evolution of neutron concentration.

It is convenient to introduce now the following relaxation rates:

$$\Gamma_{p \rightarrow n} = \Gamma_{pe \rightarrow nv} + \Gamma_{pv \rightarrow ne}, \Gamma_{n \rightarrow p} = \Gamma_{nv \rightarrow pe} + \Gamma_{ne \rightarrow pv}, \quad (42)$$

Then the kinetic equation for the neutron concentration  $X_n$  can be written as

$$\begin{aligned} \frac{dX_n}{dt} &= X_p \Gamma_{p \rightarrow n} - X_n (\Gamma_{n \rightarrow p} + \Gamma_n), \\ &= (1 - X_n) \Gamma_{p \rightarrow n} - X_n (\Gamma_{n \rightarrow p} + \Gamma_n), \\ &= \Gamma_{p \rightarrow n} - X_n (\Gamma_{p \rightarrow n} + \Gamma_{n \rightarrow p} + \Gamma_n). \end{aligned} \quad (43)$$

The first approximation we can make to solve Eq. (43) by assuming that the universe is expanding very slowly and there can be instantaneous kinetic detailed balance equilibrium in the particle yields; this is the ‘adiabatic’ approximate solution found setting  $dX_n/dt = 0$  in Eq. (43); it applies in the domain we called thermal equilibrium above. If neutron would not decay  $X_n^{ad}$  would indeed be exactly the thermal result Eq. (23). However, solving with decay rate we obtain the instantaneous detailed balance result

$$X_n^{ad} = \frac{1}{1 + \Gamma_{n \rightarrow p} / \Gamma_{p \rightarrow n} + \Gamma_n / \Gamma_{p \rightarrow n}}. \quad (44)$$

The adiabatic solution arises from the competition between neutron production, weak interaction conversion, and decay rates, yielding the modified equilibrium neutron concentration.

It is important to note that in the ratios of  $\Gamma$ s seen in Eq. (44) the strength of weak interactions cancels out exactly, the adiabatic result just like the thermal equilibrium result depends on phase space size of different processes only. This solution  $X_n^{ad}$  is shown as dashed line in Fig. 4, and on linear scale it agrees with the thermal equilibrium result  $X_n^{th}$  also shown as overlay green dotted line. Any deviation could be only expected in low temperature domain as one sees looking in depth at reaction rates in Fig. 3. Indeed we see this in the insert in Fig. 4 showing  $X_n^{th} / X_n^{ad}$ .

We now obtain the correction to the adiabatic neutron concentration  $X_n^{ad}$ . The kinetic equation of neutron concentration can be used in the format

$$\frac{dX_n}{dt} + (\Gamma_{p \rightarrow n} + \Gamma_{p \rightarrow n} + \Gamma_n) (X_n - X_n^{ad}) = 0. \quad (45)$$

Adopting the solution method from paper [7], the general solution can be written

$$\begin{aligned} X_n(y) &= X_n^{ad}(y) - \int_{y_0}^y dy' I(y, y') \frac{dX_n^{ad}(y')}{dy'}, \\ &= X_n^{ad}(y) + X_n^{corr}(y), \quad y \equiv Q/T, \end{aligned} \quad (46)$$

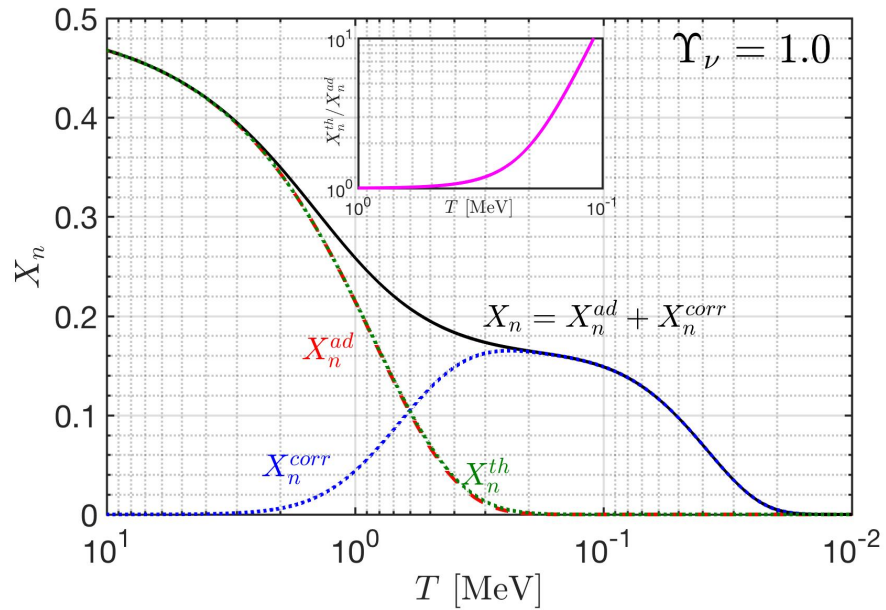


**Figure 4.** The neutron concentration  $X_n$  as a function of temperature. Dashed line: Result obtained under assumption that WI dominate Hubble expansion. Green dotted line: corresponds to thermal equilibrium, it is hard to see a difference but in the ratio  $X_n^{th}/X_n^{ad}$  seen in the insert. Blue dotted line: Correction to dashed line arising allowing kinetic neutron abundance processes and Hubble expansion. Solid line: The concentration of neutrons in the Universe. Results obtained for standard WI reaction constant and as indicated by  $Y_\nu = 1$  for chemically equilibrated (free streaming) neutrino background.

where the function  $I(y, y')$  is

$$I(y, y') = \exp \left[ - \int_{y'}^y \frac{dy''}{y''} \frac{(\Gamma_{p \rightarrow n} + \Gamma_{p \rightarrow n} + \Gamma_n)}{H} \right]. \quad (47)$$

The Hubble expansion rate competes with the WI reaction rate in the function  $I(y, y')$ .

The correction term Eq. (46) is seen as a dotted line in Fig. 4. The combined result, the neutron concentration as a function of temperature in primordial Universe, is the solid line. The neutron concentration follows the adiabatic solution for high temperatures where WI reactions remain dominant. As the Hubble expansion rate competes with WI reaction rates, the neutron concentration is dominated by kinetic processes only. In between there is a domain of transition. Towards the end of the BBN temperature range  $X_n$  decreases toward zero since the neutron decay becomes the dominant process.

Before, and at the onset of the BBN period the neutron concentration, without here allowing for nuclear fusion reactions that deplete neutrons, is determined by the ratio of the total WI reaction rate to the Hubble expansion rate, see Eq. (47). Consequently  $X_n$  via correction term depends on magnitude of  $G_F$ . It is clear by inspection that the simple freeze-out+lifetime neutron decay model can create an approximation as follows: Taking a high freeze-out condition near  $T = 2$  MeV in disagreement with actual values seen in Fig. 3 we minimize the correction term. The neutron decay shape (compare shape at low  $T$ ) is than a good fit. However, the yield shoulder below  $T = 30$  keV will be missed. The results shown in Fig. 4 were obtained without allowing for nuclear fusion reactions which deplete neutron concentration as well.

In the top frame of Fig. 5 we show neutron concentration  $X_n$  as a function of temperature with different values of Weinberg angle  $s_W$  and in the bottom frame we show the ratio

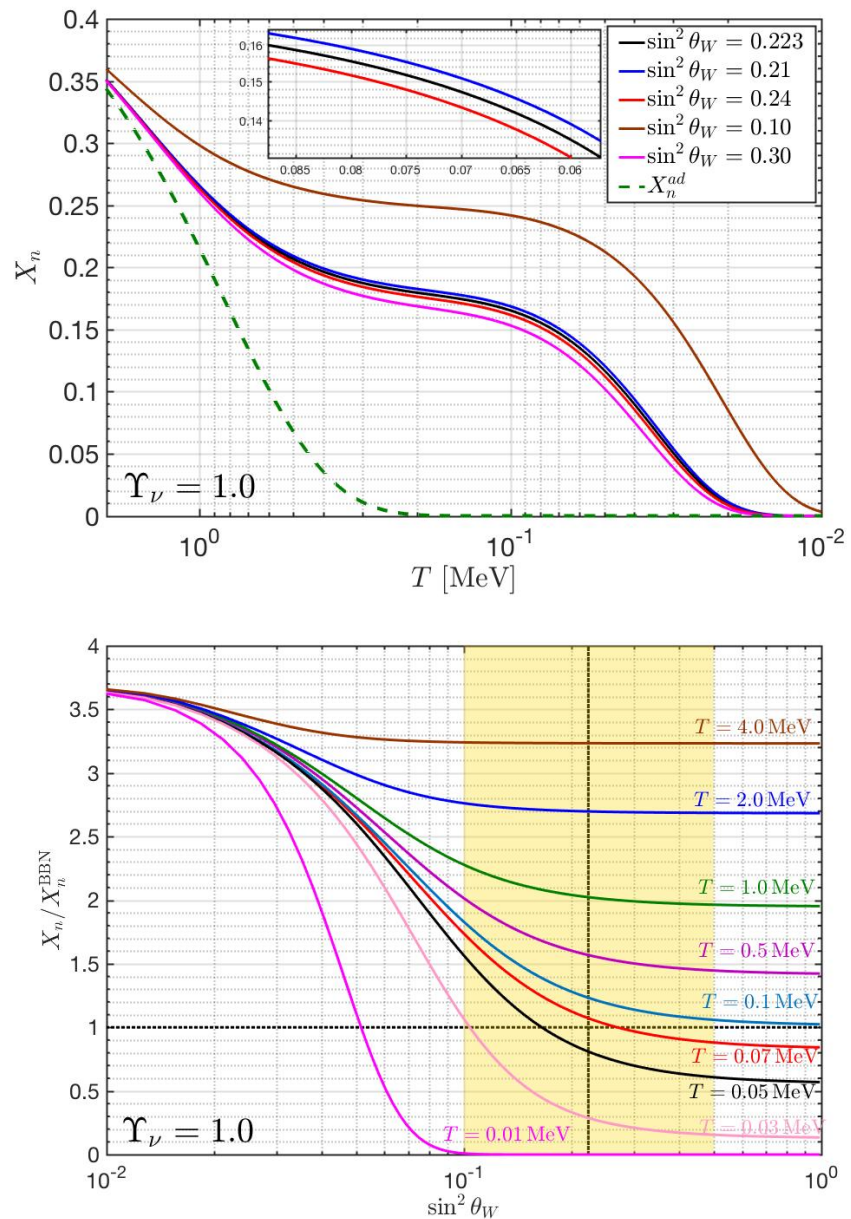


**Figure 5. Top frame:** The neutron concentration  $X_n$  as a function of temperature  $T$  with different values of Weinberg angle  $s_W$  and assumed chemical equilibrium of background neutrinos,  $Y_\nu = 1$ . The cases  $s_W = 0.1$  and  $s_W = 0.3$  illustrate the range of the Weinberg angle for which the approximation in Eq. (6) remains valid. The insert amplifies variation of neutron concentration for temperature characteristic of BBN onset and small variation of  $s_W$  from standard value as we considered before. There is no dependence on  $s_W$  in the adiabatic component (dashed line); **Bottom frame:** The normalized neutron concentration  $X_n / X_n^{BBN}$  as a function of Weinberg angle  $s_W$  for different temperature values with chemical equilibrium neutrino fugacity  $Y_\nu = 1$ . We can track as a function of  $s_W$  the change in value  $X_n^{BBN} = 0.13$  (horizontal black dotted line). The vertical black dotted line marks the adopted CODATA value  $s_W = 0.223$ . The yellow region indicates the range of the Weinberg angle for which the approximation in Eq. (6) is valid.

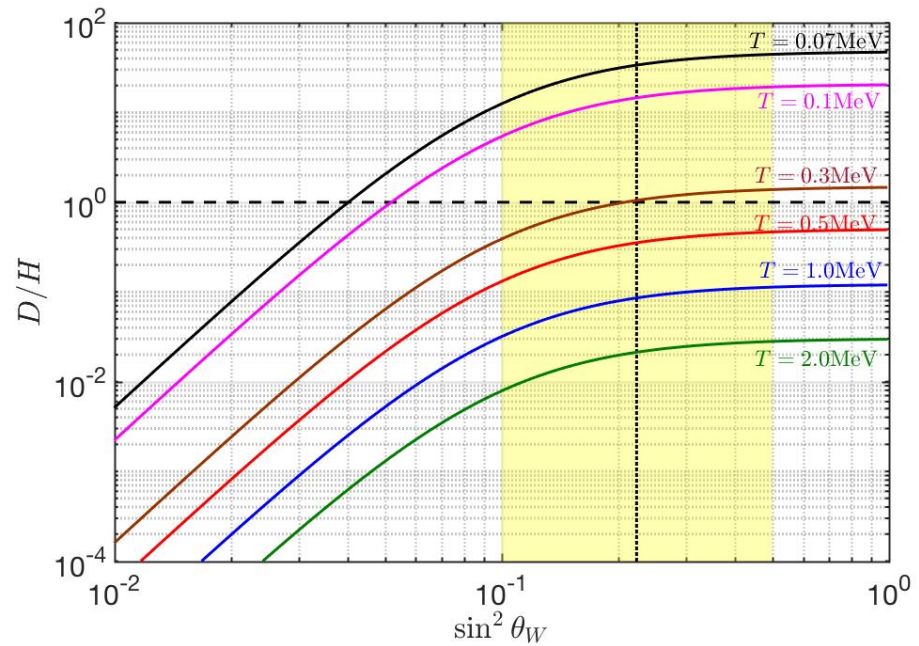


**Figure 6.** The ratio between weak interaction reaction constant  $D$ , Eq. (15) and the Hubble parameter as a function of the Weinberg angle  $s_W$  for temperature values  $T = 2, 1, 0.5, 0.3, 0.1, 0.07$  MeV. The horizontal dotted line shows  $D = H$ , and the vertical dotted line marks the Standard Model value  $s_W = 0.223$ . The yellow region indicates where we can expect approximation in Eq. (6) to be valid.

of the neutron concentration  $X_n$  to the standard BBN value  $X_n^{\text{BBN}} = 0.13$  (black dotted line) as a function of the Weinberg angle  $s_W$  for different temperatures. At high temperatures, the neutron fraction exhibits only a weak dependence on variations in the weak mixing angle as we expect, since the abundance follows the kinetic detailed balance ‘adiabatic’ result which does not depend on the strength of  $G_F$ . In contrast, at lower temperatures the neutron concentration  $X_n$  becomes strongly sensitive to the value of the Weinberg angle. The neutron concentration  $X_n$  decreases as  $s_W$  increases. In particular, near the BBN temperature regime, small variations of the Weinberg angle in the range  $0.1 < s_W < 0.5$  lead to substantial changes in  $X_n$ , indicating a strong sensitivity to electro-weak parameters.

To better explain the sensitivity of the neutron concentration  $X_n$  to the value of  $G_F$ , we present in Fig 6 the ratio of the WI coupling parameter  $D$  to the Hubble parameter as a function of Weinberg angle  $s_W$  with different temperature values. The results show that near the weak interaction freeze-out temperature, this ratio is sensitive to variations in  $s_W$  and thus the neutron concentration at BBN epoch is affected. To accurately capture these effects, it is necessary to study the kinetic evolution of the neutron yield for a range of  $s_W$  near to the reference value we adopted  $s_W = 0.223$ .

## 5. Conclusions and Discussion

We have described in Section 4 the competition between the Hubble expansion speed and the kinetic reactions processes responsible for the detailed value of the neutron abundance before and at onset of BBN. The ‘adiabatic limit’ generalizes the thermal approximation. Since the strength of weak interactions, the Fermi constant  $G_F^2$ , cancels in the ratio between different electro-weak rates the result is solely dependent on phase space size, this is the detailed balance neutron concentration. The detailed balance differs from thermal equilibrium abundance since we are allowing also for the decay of neutrons.

To obtain the kinetic neutron concentration  $X_n$  we note that several key WI reaction rates seen in Fig. 3 intersect near to  $T$  of interest in BBN. This implies that the neutron freeze-out and decay rates are interwoven with the Hubble expansion rate. The outcome of gradual change of  $X_n$  is illustrated for the vacuum SM parameters in Fig. 4.

We then proceed to discuss and present in quantitative terms the variation of neutron concentration preceding the BBN as a function of  $s_W$ , see Fig. 5. It is in this new context that small changes in weak interaction strength driven by Weinberg angle can have impact on neutron abundance available in BBN epoch. We have shown that the precision BBN which requires  $X_n$  at sub percentile level depends on value of  $s_W$  or equivalently  $G_F$  in the hot BBN plasma environment.

The results for  $X_n$  also depend on precision knowledge of the Hubble expansion parameter during the BBN period. We have been working to develop this understanding for a long time [8]. We present our sophisticated model as a reference for convenience of the reader in the Appendix A. In our approach, following on neutrino decoupling, the transfer of entropy and reheating of photons by  $e^\pm$ -pair annihilation is gradual, obtained from the instantaneous thermal  $e^\pm$ -pair abundance as a function of temperature. Our precise description has non-negligible improvements compared to some other BBN models.

Looking forward to further work and impact of our results:

- **BBN:** In the presence of ongoing BBN nuclear reactions in addition to the neutron loss by decay, neutrons are ‘lost’ to the produced nuclei, for most part in net photoproduction of deuterons: Our formulation remains valid in principle, as introducing additional nuclear reaction rate loss (and gain) terms aside of  $\Gamma_n$  in Eq. (47) we allow for the loss of neutrons due to nuclear reactions such as photoproduction of deuterons,  $n + p \rightarrow d + \gamma$ . The importance of this remark is that the production of neutrons by WI process  $\Gamma_{p \rightarrow n}$  continues to replenish to some degree such small losses as is implied by the result seen in Fig. 4.
- **Weinberg symmetry breaking:** We offered results for  $X_n$  motivating future study of unexplored phenomena in electro-weak physics addressing the question if the value of  $s_W$  and thus  $G_F$  could be sensitive to environmental factors. In the primordial Universe we suggested the need for the establishment of the temperature dependence of  $s_W$  and thus  $G_F$ . This clearly requires considerable theoretical effort. We further noted that the observed discrepancies in laboratory measured neutron lifetime measurements could be interpreted in terms of variation of  $s_W$  and thus  $G_F$  as a function of so far not considered experimental environment. This is in part motivated by relatively large scatter of measured values of  $s_W$ . We noted that this variance in  $s_W$  exceeds by a factor 8 the variation required to understand the measured neutron lifetime disagreements.

## Author Contributions

Article was created in collaboration, with both authors contributing equally.

## Funding

This research received no external funding.

## Acknowledgments

We thank Bernhard Lauss (PSI-Villigen) for valuable comments.

## Conflicts of Interest

The authors declare no conflict of interest.

## Appendix A Hubble Parameter and Photon Reheating

In this section, we summarize the key theoretical background relevant to our analysis and in particular the detailed value of the Hubble parameter  $H$  in the primordial Universe. Much of the material is based on the review [8], which discusses the connection between particle physics and the primordial-Universe cosmology.

In the epoch of interest,  $10 \text{ MeV} > T > 0.01 \text{ MeV}$ , the Universe is dominated by radiation and effectively massless matter behaving like radiation. The Hubble parameter can be written as

$$H^2 = \frac{8\pi G_{\text{N}}}{3}(\rho_\gamma + \rho_{e^\pm} + \rho_\nu), \quad (\text{A1})$$

where  $\rho_i$  is the energy density for  $\gamma, e^\pm, \nu$ . It is convenient to rewrite the sum of energy density of relativistic species in terms of photo energy density, we have

$$\rho_{\text{R}} = \sum_i \rho_i = \frac{\pi^2}{30} g_* T^4, \quad (\text{A2})$$

where  $g_*$  counts the effective number of ‘energy’ degrees of freedom, we have

$$g_* = \sum_{i=\text{bosons}} g_i \left( \frac{T_i}{T_\gamma} \right)^4 B + \frac{7}{8} \sum_{i=\text{fermions}} g_i \left( \frac{T_i}{T_\gamma} \right)^4 F. \quad (\text{A3})$$

The functions  $B$  and  $F$  are defined as

$$B = \frac{15}{\pi^4} \int_{m_i/T}^{\infty} dx \sqrt{x^2 - \left( \frac{m_i}{T} \right)^2} \frac{x^2}{e^x - 1}, \quad (\text{A4})$$

$$F = \frac{8}{7} \times \frac{15}{\pi^4} \int_{m_i/T}^{\infty} dx \sqrt{x^2 - \left( \frac{m_i}{T} \right)^2} \frac{x^2}{e^x + 1}. \quad (\text{A5})$$

In Fig. A1, we show the effective number of energy degrees of freedom  $g_*$  as a function of temperature. The red dashed line shows the contribution from photons, neutrinos, and massless electrons/positrons, while the blue dashed line represents the contribution from photons and cold neutrinos. In Fig. A2, we plot the Hubble parameter as a function of temperature from  $10 \geq T \geq 0.01 \text{ MeV}$  in the primordial Universe. It shows that the transition between Hubble parameter from contributions by photons, neutrinos, and massless electrons/positrons to contributions from only photons and neutrinos is driven by the smooth disappearance of nonrelativistic  $e^\pm$ .

After neutrino freeze-out and when  $m_e \gg T$ , the  $e^\pm$  becomes non-relativistic and annihilate. In this case, their entropy is transferred to the other relativistic particles still present in the cosmic plasma, *i.e.* photons, resulting in an increase in photon temperature as compared to the freestreaming neutrinos. From entropy conservation we have

$$\frac{2\pi}{45} g_*^s(T_k) T_k^3 V_k + S_\nu(T_k) = \frac{2\pi}{45} g_*^s(T) T^3 V + S_\nu(T), \quad (\text{A6})$$

where we use the subscripts  $k$  to denote quantities for neutrino freeze-out and  $g_*^s$  counts the degree of freedom for relativistic species in primordial Universe. The effective number of ‘entropy’ degrees of freedom can be written as

$$g_*^s = \sum_{i=\text{bosons}} g_i \left( \frac{T_i}{T_\gamma} \right)^3 B^s + \frac{7}{8} \sum_{i=\text{fermions}} g_i \left( \frac{T_i}{T_\gamma} \right)^3 F^s, \quad (\text{A7})$$

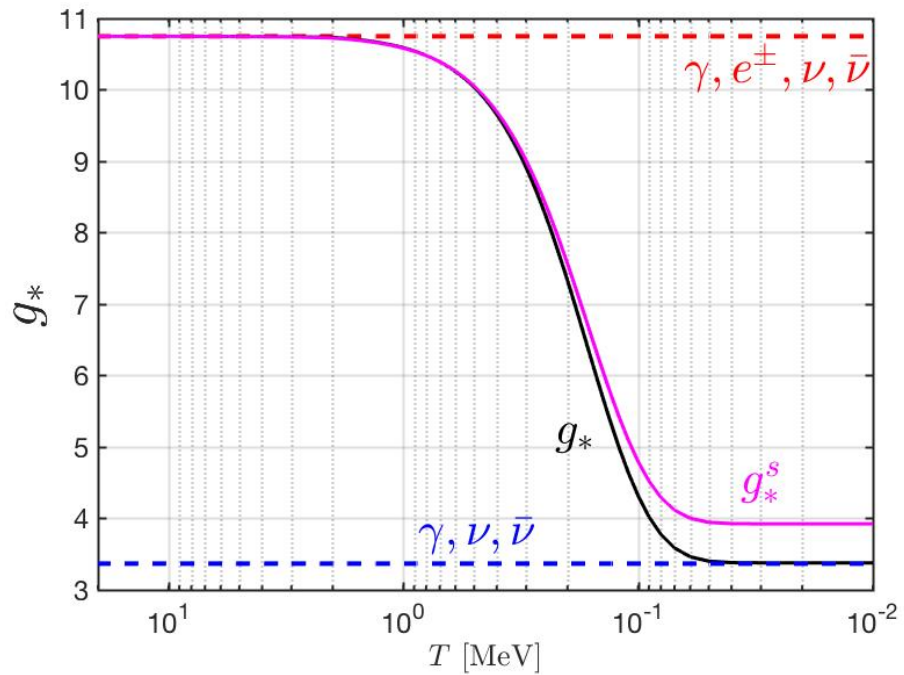


**Figure A1.** The effective number of ‘energy’ degrees of freedom  $g_*$  as a function of temperature. The red dashed line represents the degrees of freedom from photon, neutrino, and massless electron/positron. The blue dashed line labels the degree of freedom for photon, and cold neutrino.

where the functions  $B^s(m_i/T)$  and  $F^s(m_i/T)$  are defined as

$$B^s = \frac{45}{12\pi^4} \int_{m_i/T}^{\infty} dx \frac{\sqrt{x^2 - (m_i/T)^2} [4x^2 - (m_i/T)^2]}{e^x - 1}, \quad (\text{A8})$$

$$F^s = \frac{8}{7} \times \frac{45}{12\pi^4} \int_{m_i/T}^{\infty} dx \frac{\sqrt{x^2 - (m_i/T)^2} [4x^2 - (m_i/T)^2]}{e^x + 1}. \quad (\text{A9})$$

After neutrino freeze-out, their entropy is conserved independently and the temperature can be written as

$$T_\nu \equiv \frac{a(t_k)}{a(t)} T_k = \left( \frac{V_k}{V} \right)^{1/3} T_k. \quad (\text{A10})$$

In this case, from entropy conservation, Eq. (A6), we obtain the neutrino temperature

$$T_\nu = \frac{T}{\kappa}, \quad \kappa \equiv \left[ \frac{g_*^s(T_k)}{g_*^s(T)} \right]^{1/3}. \quad (\text{A11})$$

For neutrinos, after neutrino/antineutrino kinetic freeze-out they become free streaming particles. If we assume that kinetic freeze-out occurs at some time  $t_k$  and temperature  $T_k$ , then for  $t > t_k$  the free streaming distribution function can be written as [31]

$$f_\nu = \frac{1}{Y_\nu^{-1} \exp \left( \sqrt{\frac{E^2 - m_\nu^2}{T_\nu^2} + \frac{m_\nu^2}{T_k^2} + \frac{\mu_\nu}{T_k}} \right) + 1}, \quad (\text{A12})$$

for antineutrinos. In our calculation, we assume the condition  $T_k = 2 \text{ MeV} \gg \mu_{\bar{\nu}}, m_\nu$ , *i.e.* we consider the massless neutrino in plasma.

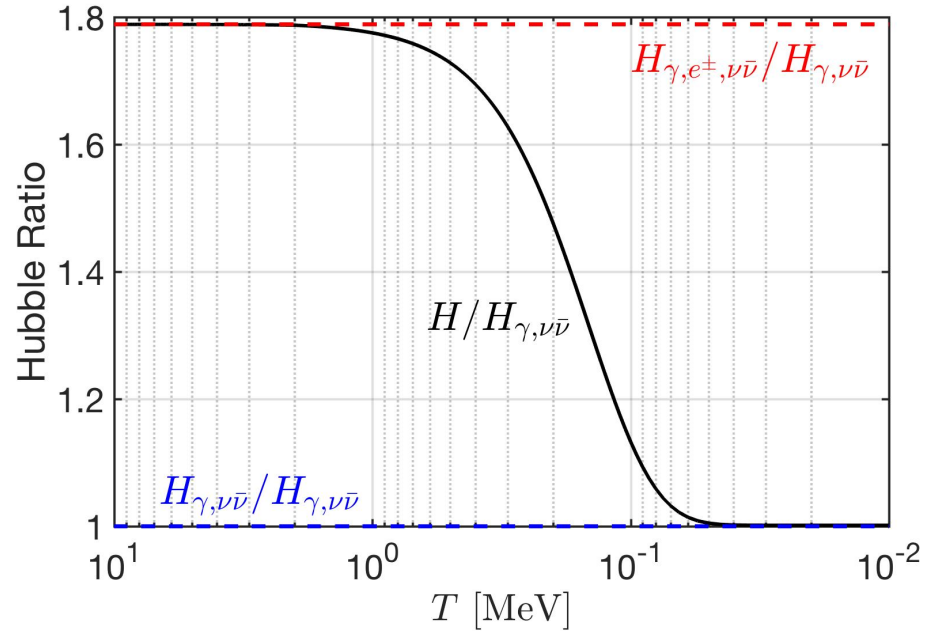


**Figure A2.** The ratio between Hubble parameter as a function of temperature from  $10 \geq T \geq 0.01 \text{ MeV}$  in the primordial Universe. It shows that the transition between Hubble parameter from contributions by photons, neutrinos, and massless electrons/positrons to contributions from only photons and neutrinos is driven by the smooth disappearance of nonrelativistic  $e^{\pm}$ .

## References

1. J. P. Uzan, “Fundamental constants: from measurement to the universe, a window on gravitation and cosmology,” *Living Rev. Rel.* **28**, no.1, 6 (2025) doi:10.1007/s41114-025-00059-y [arXiv:2410.07281 [astro-ph.CO]].
2. D. Milaković and J. K. Webb, “Beyond  $\Lambda$ CDM: fundamental constants as cosmological observables,” *White Paper submitted to ESO’s Expanding Horizons initiative*, doi:10.48550/arXiv.2602.10987 [arXiv:2602.10987 [astro-ph.CO]].
3. J. Birrell, C. T. Yang and J. Rafelski, “Relic Neutrino Freeze-out: Dependence on Natural Constants,” *Nucl. Phys. B* **890**, 481-517 (2014) doi:10.1016/j.nuclphysb.2014.11.020 [arXiv:1406.1759 [nucl-th]].
4. S. P. Martin, “Three-loop corrections to the Fermi decay constant in the  $\overline{\text{MS}}$  scheme,” *Phys. Rev. D* **112**, no.7, 073002 (2025) doi:10.1103/physrevd.112.073002 [arXiv:2507.15946 [hep-ph]].
5. M. J. G. Veltman, “Limit on Mass Differences in the Weinberg Model,” *Nucl. Phys. B* **123**, 89-99 (1977) doi:10.1016/0550-3213(77)90342-X
6. S. Navas *et al.* [Particle Data Group], “Review of particle physics,” *Phys. Rev. D* **110**, no.3, 030001 (2024) doi:10.1103/PhysRevD.110.030001
7. J. Bernstein, L. S. Brown and G. Feinberg, “Cosmological Helium Production Simplified,” *Rev. Mod. Phys.* **61**, 25 (1989) doi:10.1103/RevModPhys.61.25.
8. J. Rafelski, J. Birrell, C. Grayson, A. Steinmetz and C. T. Yang, “Quarks to Cosmos: Particles and Plasma in Cosmological Evolution,” *Eur. Phys. J. ST* **234**, no.7, 1125-1329 (2025) doi:10.1140/epjs/s11734-025-01470-w [arXiv:2409.19031 [hep-ph]].
9. S. R. Coleman and E. J. Weinberg, “Radiative Corrections as the Origin of Spontaneous Symmetry Breaking,” *Phys. Rev. D* **7**, 1888-1910 (1973) doi:10.1103/PhysRevD.7.1888.
10. A. Sirlin and A. Ferroglia, “Radiative Corrections in Precision Electroweak Physics: a Historical Perspective,” *Rev. Mod. Phys.* **85**, no.1, 263-297 (2013) doi:10.1103/RevModPhys.85.263 [arXiv:1210.5296 [hep-ph]].
11. G. Gwinner and L. A. Orozco, “Studies of the weak interaction in atomic systems: towards measurements of atomic parity non-conservation in francium,” *Quantum Sci. Technol.* **7**, no.2, 024001 (2022) doi:10.1088/2058-9565/ac4424.

12. R. Aaij *et al.* [LHCb], “Measurement of the effective leptonic weak mixing angle,” *JHEP* **12**, 026 (2024) doi:10.1007/JHEP12(2024)026 [arXiv:2410.02502 [hep-ex]].
13. A. Hayrapetyan *et al.* [CMS], “Measurement of the Drell–Yan forward-backward asymmetry and of the effective leptonic weak mixing angle in proton-proton collisions at  $\sqrt{s}=13\text{TeV}$ ,” *Phys. Lett. B* **866**, 139526 (2025) doi:10.1016/j.physletb.2025.139526 [arXiv:2408.07622 [hep-ex]].
14. P. Mohr, E. Tiesinga, D. Newell, and B. Taylor, (2024), “Codata Internationally Recommended 2022 Values of the Fundamental Physical Constants,” [online], [https://tsapps.nist.gov/publication/get\\_pdf.cfm?pub\\_id=958002](https://tsapps.nist.gov/publication/get_pdf.cfm?pub_id=958002), <https://physics.nist.gov/constants> (Accessed February 17, 2026).
15. V. Tishchenko *et al.* [MuLan] “Detailed Report of the MuLan Measurement of the Positive Muon Lifetime and Determination of the Fermi Constant,” *Phys. Rev. D* **87**, no.5, 052003 (2013) doi:10.1103/PhysRevD.87.052003 [arXiv:1211.0960 [hep-ex]].
16. A. Sirlin, “Radiative Corrections in the SU(2)-L x U(1) Theory: A Simple Renormalization Framework,” *Phys. Rev. D* **22**, 971-981 (1980) doi:10.1103/PhysRevD.22.971
17. J. Erler and P. Langacker, “electro-weak model and constraints on new physics,” in: *2004 Review of Particle Physics*, *Phys. Lett. B* **592** 1 (2004) [arXiv:hep-ph/0407097 [hep-ph]].
18. M. Consoli, W. Hollik and F. Jegerlehner, “The Effect of the Top Quark on the M(W)-M(Z) Interdependence and Possible Decoupling of Heavy Fermions from Low-Energy Physics,” *Phys. Lett. B* **227**, 167-170 (1989) doi:10.1016/0370-2693(89)91301-4.
19. D. H. Wilkinson, “Analysis of Neutron Beta Decay,” *Nucl. Phys. A* **377**, 474 (1982). doi:10.1016/0375-9474(82)90051-3.
20. A. Czarnecki, W. J. Marciano and A. Sirlin, “Neutron Lifetime and Axial Coupling Connection,” *Phys. Rev. Lett.* **120**, 202002 (2018) doi:10.1103/PhysRevLett.120.202002 [arXiv:1802.01804 [hep-ph]].
21. W. J. Marciano, “Fundamental Neutron Physics,” *Phys. Procedia* **51**, 19 (2014). doi:10.1016/j.phpro.2013.12.006.
22. W. J. Marciano and A. Sirlin, “Improved calculation of electro-weak radiative corrections and the value of  $V(\text{ud})$ ,” *Phys. Rev. Lett.* **96**, 032002 (2006) doi:10.1103/PhysRevLett.96.032002 [hep-ph/0510099].
23. A. Czarnecki, W. J. Marciano and A. Sirlin, “Precision measurements and CKM unitarity,” *Phys. Rev. D* **70**, 093006 (2004) doi:10.1103/PhysRevD.70.093006 [hep-ph/0406324].
24. A. T. Yue, M. S. Dewey, D. M. Gilliam, G. L. Greene, A. B. Laptev, J. S. Nico, W. M. Snow and F. E. Wietfeldt, “Improved Determination of the Neutron Lifetime,” *Phys. Rev. Lett.* **111**, no.22, 222501 (2013) doi:10.1103/PhysRevLett.111.222501 [arXiv:1309.2623 [nucl-ex]].
25. F. E. Wietfeldt, “The Neutron Lifetime Discrepancy and Its Implications for Cosmology and Dark Matter,” *Symmetry* **16**, no.8, 956 (2024) doi:10.3390/sym16080956.
26. R. V. Wagoner, W. A. Fowler and F. Hoyle, “On the Synthesis of elements at very high temperatures,” *Astrophys. J.* **148**, 3-49 (1967) doi:10.1086/149126.
27. C. T. Yang, J. Birrell and J. Rafelski, “Temperature Dependence of the Neutron Lifetime,” [arXiv:1805.06543 [nucl-th]].
28. C. Pitrou, A. Coc, J. P. Uzan and E. Vangioni, “Precision big bang nucleosynthesis with improved Helium-4 predictions,” *Phys. Rept.* **754**, 1-66 (2018) doi:10.1016/j.physrep.2018.04.005 [arXiv:1801.08023 [astro-ph.CO]].
29. I. Kuznetsova and J. Rafelski, “Unstable Hadrons in Hot Hadron Gas in Laboratory and in the Early Universe,” *Phys. Rev. C* **82**, 035203 (2010) doi:10.1103/PhysRevC.82.035203 [arXiv:1002.0375 [hep-th]].
30. T. Chowdhury and S. Ipek, “Neutron lifetime anomaly and Big Bang nucleosynthesis,” *Can. J. Phys.* **102**, no.2, 96-99 (2024) doi:10.1139/cjp-2023-0188 [arXiv:2210.12031 [hep-ph]].
31. J. Birrell, C. T. Yang, P. Chen and J. Rafelski, “Relic neutrinos: Physically consistent treatment of effective number of neutrinos and neutrino mass,” *Phys. Rev. D* **89**, 023008 (2014) doi:10.1103/PhysRevD.89.023008 [arXiv:1212.6943 [astro-ph.CO]].